Electronic Supplementary Information

Tuning the Architectures and Luminescence Properties of Cu(I) Compounds of Phenyl and Carboranyl Pyrazoles: The impact of 2D *versus* 3D Aromatic Moieties in the ligand backbone

Joan Soldevila-Sanmartín,[a,b] Eliseo Ruiz,[c] Duane Choquesillo-Lazarte,[d] Mark E. Light,[e] Clara Viñas,[a] Francesc Teixidor,[a] Rosario Núñez,*[a] Josefina Pons,[b] José G. Planas*[a]

[a] Institut de Ciència de Materials de Barcelona, ICMAB-CSIC, Campus UAB, 08193 Bellaterra, Spain.

E-mail: jginerplanas@icmab.es, rosario@icmab.es

[b] Departament de Química, Universitat Autònoma de Barcelona, Bellaterra, 08193 Barcelona, Spain.

[c] Departament de Química Inorgànica i Orgànica and Institut de Recerca de Química Teòrica i Computacional, Universitat de Barcelona, Diagonal 645, 08028 Barcelona, Spain.

[d] Laboratorio de Estudios Cristalógraficos, IACT (CSIC-Universidad de Granada), Avda. de las Palmeras 4, Armilla, Granada, 18100, Spain.

[e] School of Chemistry, University of Southampton, Highfield, Southampton SO17 1BJ, UK.

ATR-FTIR Spectra for Ligands L2-L4

The FTIR-ATR spectrum of **L2**-**L4** show signals typical of pyrazole-containing ligands such as: [ν(C=C/C=N)$_{ar}$] (1555-1552 cm^{-1}), [δ(C=C/C=N)$_{ar}$] (1452-1416 cm^{-1}), [δ(C-H)$_{ip}$] (1061-1020 cm^{-1}) and [δ(C-H)$_{oop}$] (789-717 cm^{-1})[1]; as well as a typical broad [ν(B-H)][1] (2571-2561 cm^{-1}) attributed to carborane moieties, thus confirming their successful synthesis.

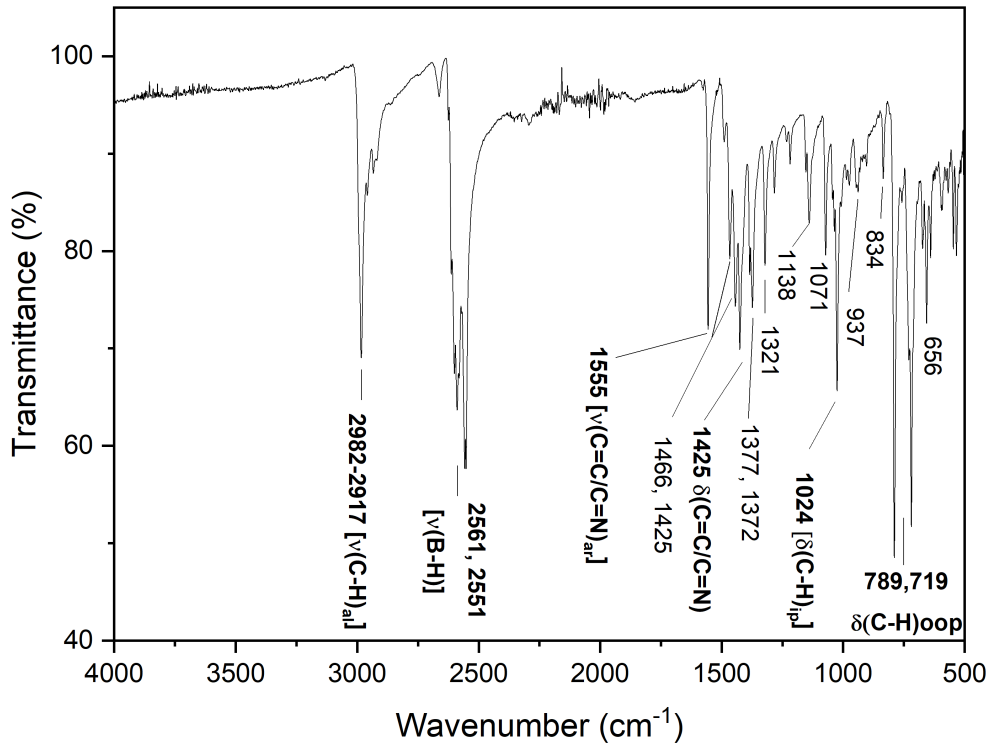

Figure S1. FTIR-ATR spectrum of **L2**.

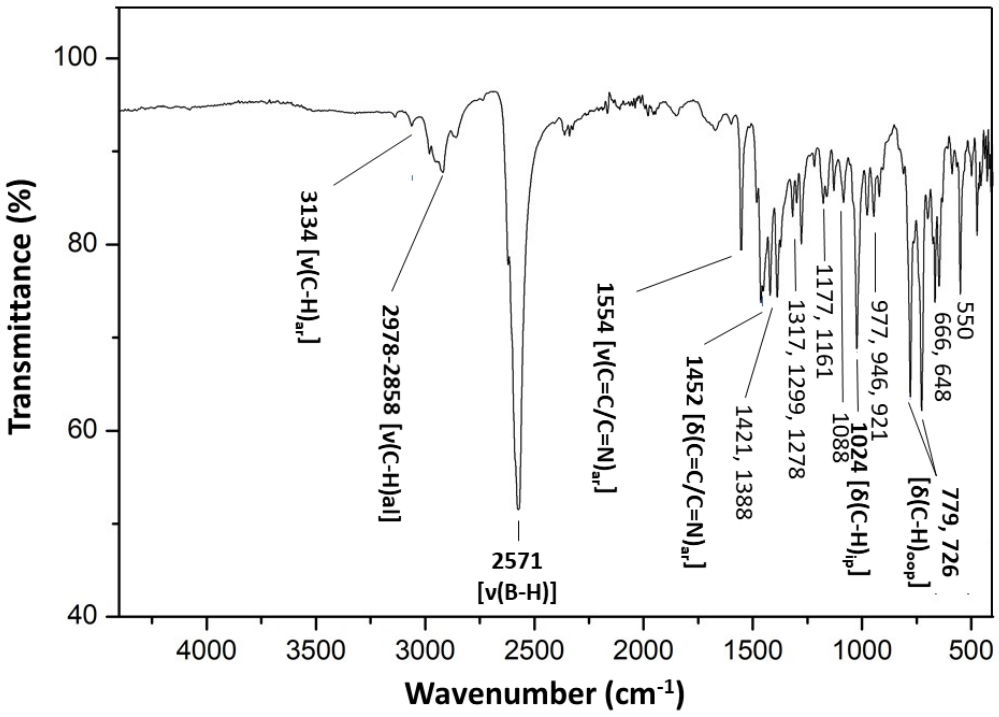

Figure S2. FTIR-ATR spectrum of **L3**.

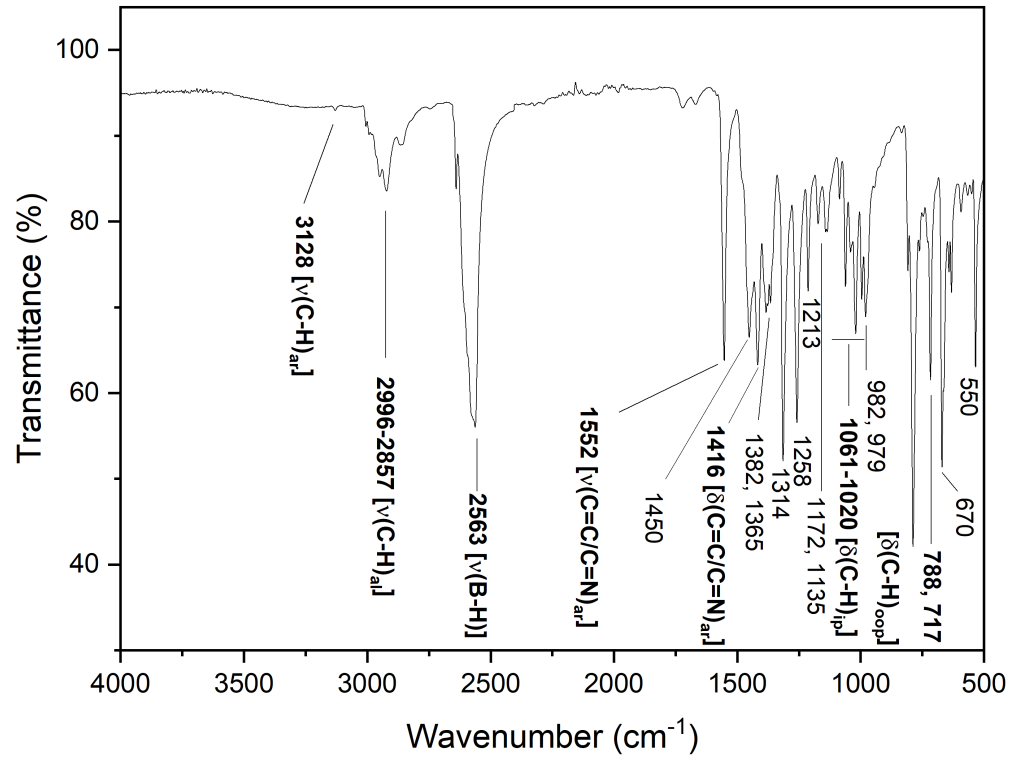

Figure S3. FTIR-ATR spectrum of **L4**.

NMR Spectra for Ligands L2-L4

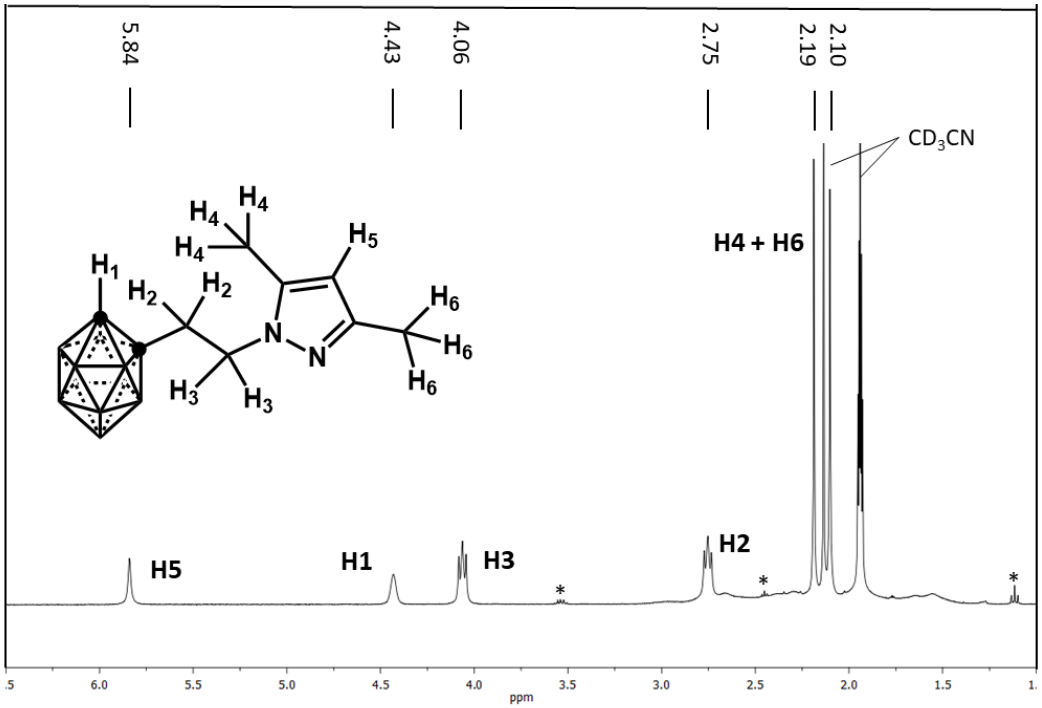

Figure S4. ^{1}H NMR spectrum of **L2** (CD_3CN, 400.0 MHz). Ethanol traces are indicated with asterisk.

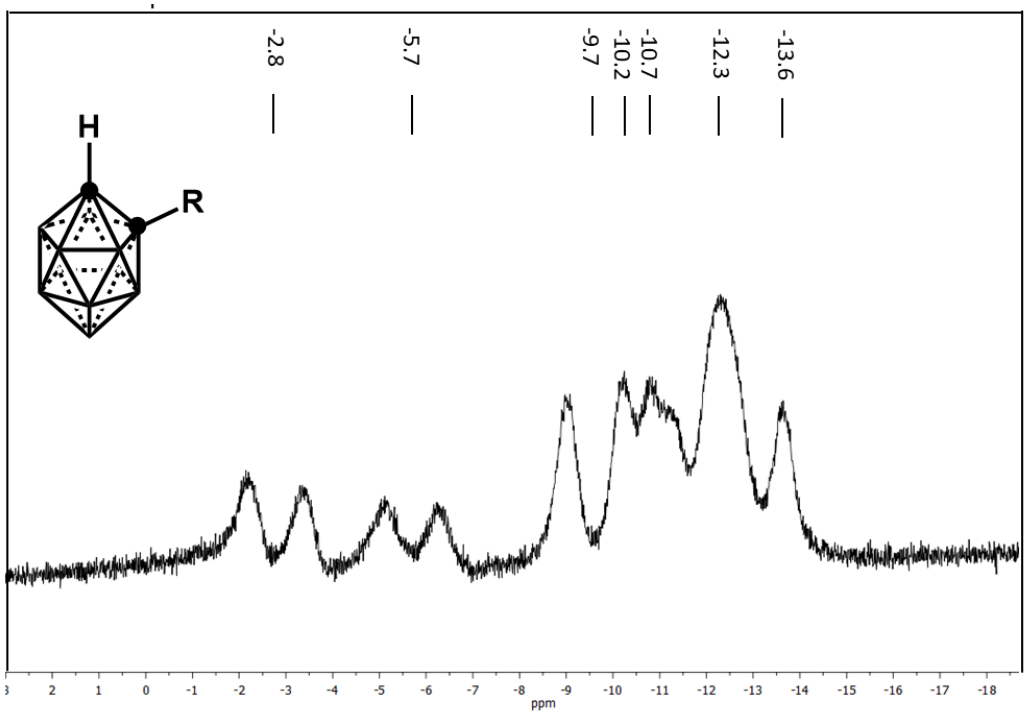

Figure S5. ^{11}B NMR spectrum of **L2** (CD_3CN, 128.6 MHz).

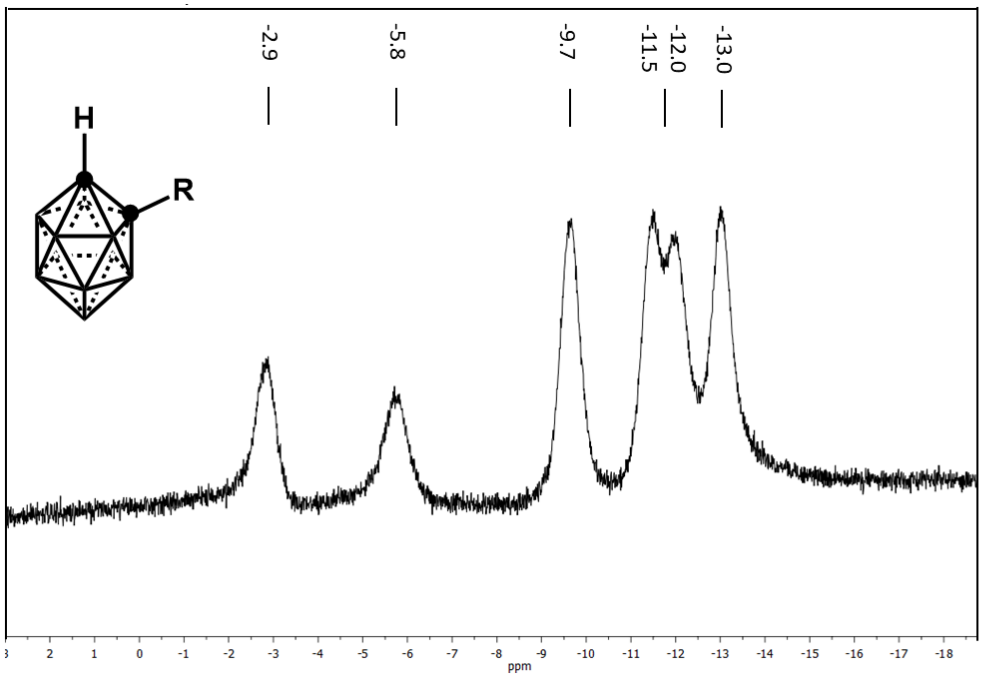

Figure S6. $^{11}B\{^{1}H\}$ NMR spectrum of **L2** (CD_3CN, 128.6 MHz).

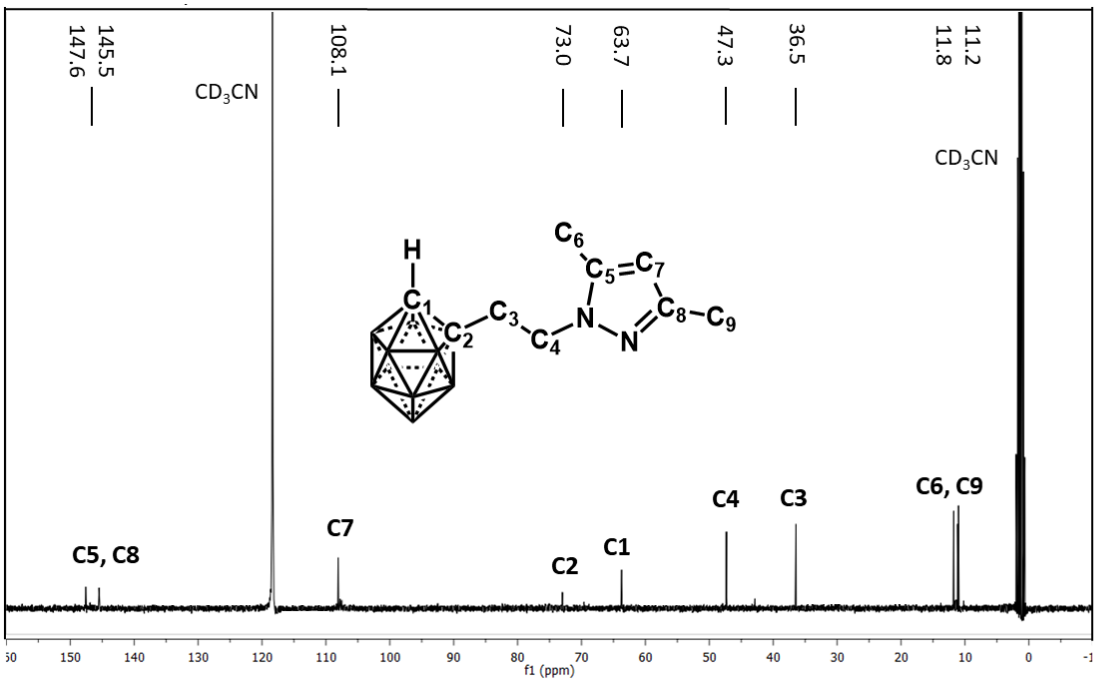

Figure S7. $^{13}C\{^{1}H\}$ NMR spectrum of **L2** (CD_3CN, 100.6 MHz).

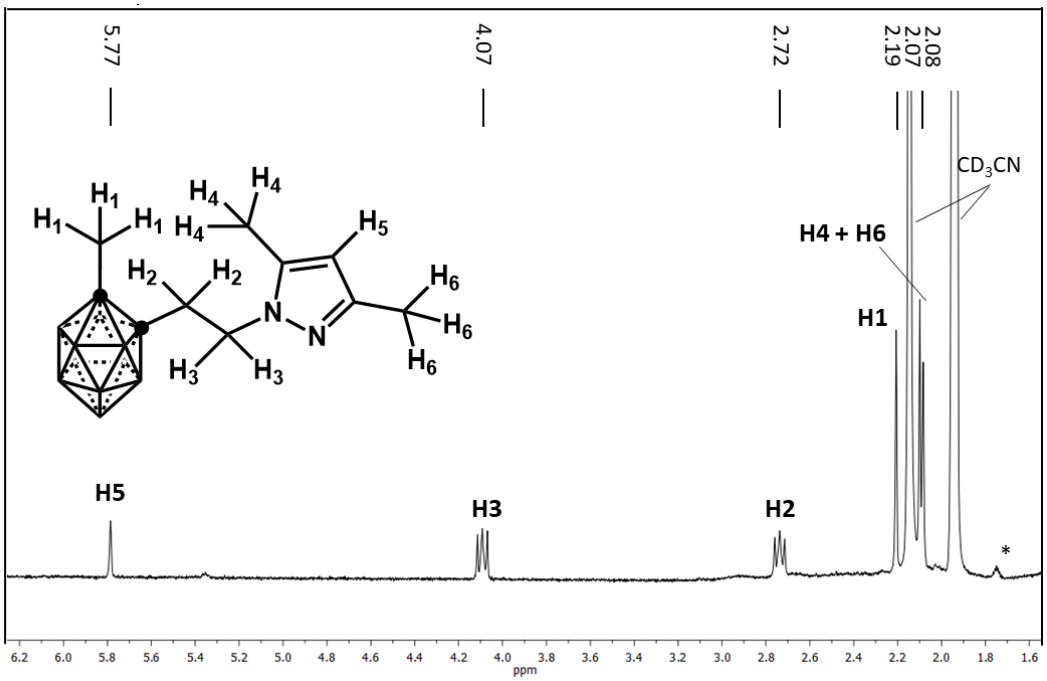

Figure S8. ^{1}H NMR spectrum of **L3** (CD_3CN, 400.0 MHz). Traces of impurities are indicated with asterisk.

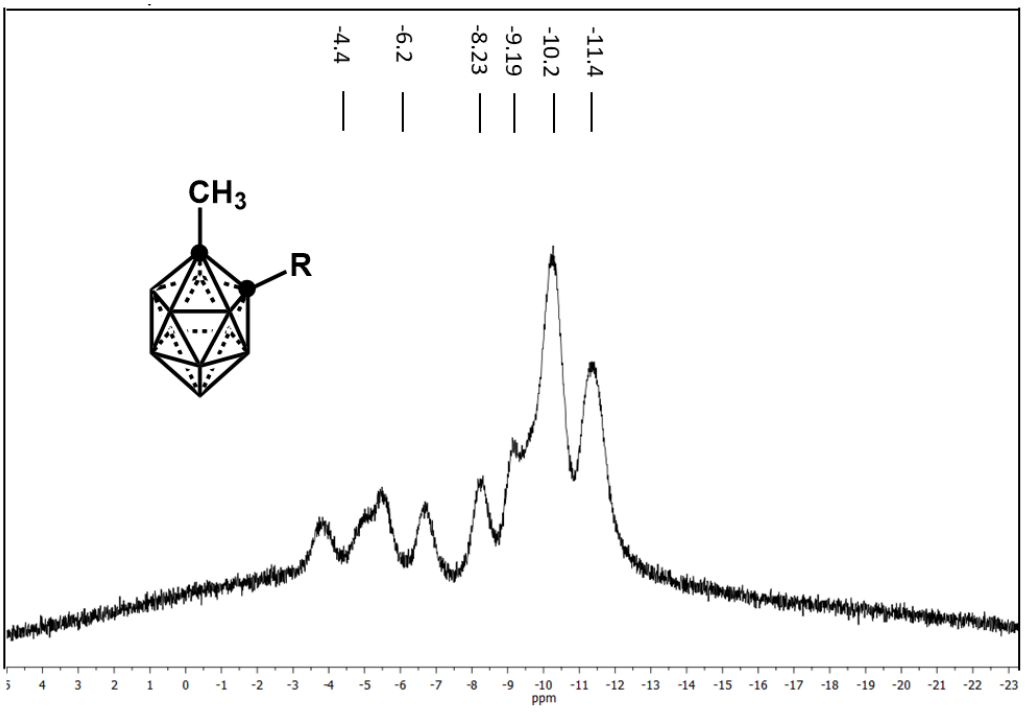

Figure S9. ^{11}B NMR spectrum of **L3** (CD_3CN, 128.6 MHz).

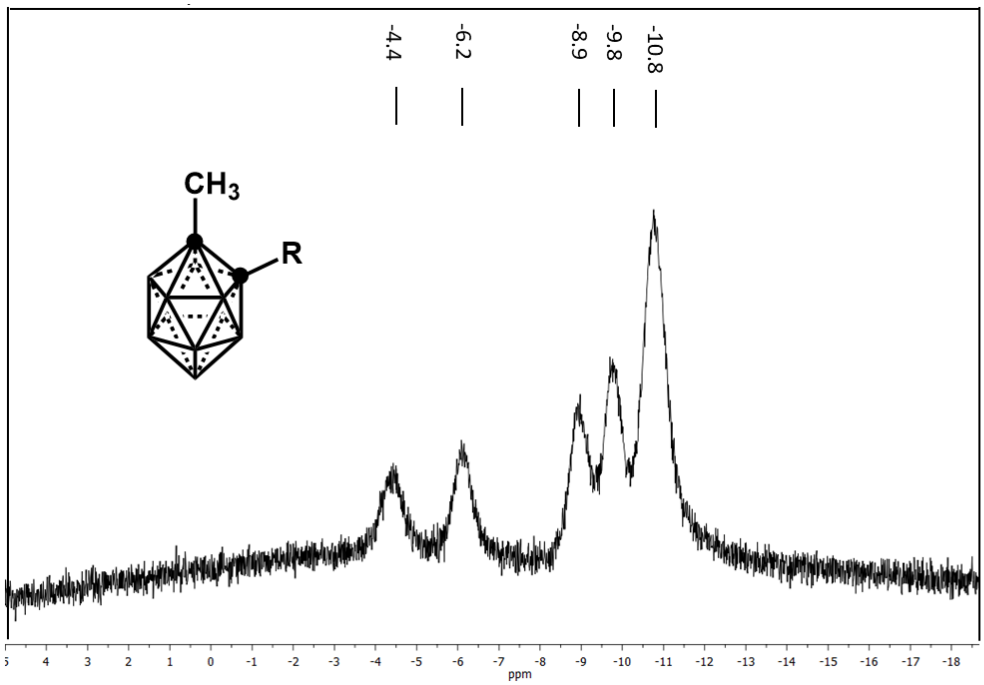

Figure S10. $^{11}B\{^{1}H\}$ NMR spectrum of **L3** (CD_3CN, 128.6 MHz).

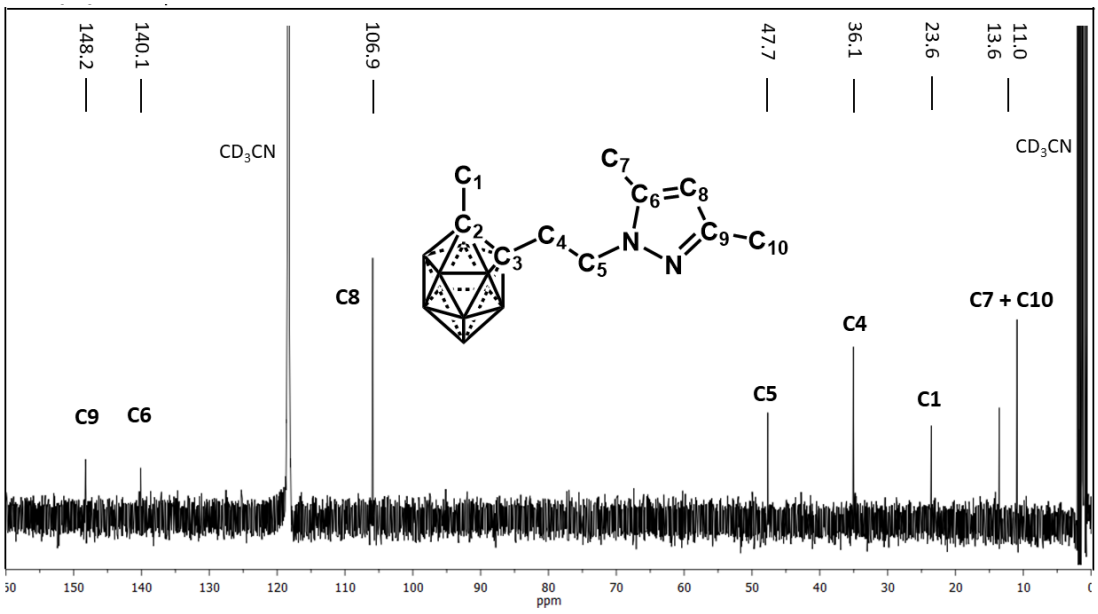

Figure S11. $^{13}C\{^{1}H\}$ NMR spectrum of **L3** (CD_3CN, 100.6 MHz).

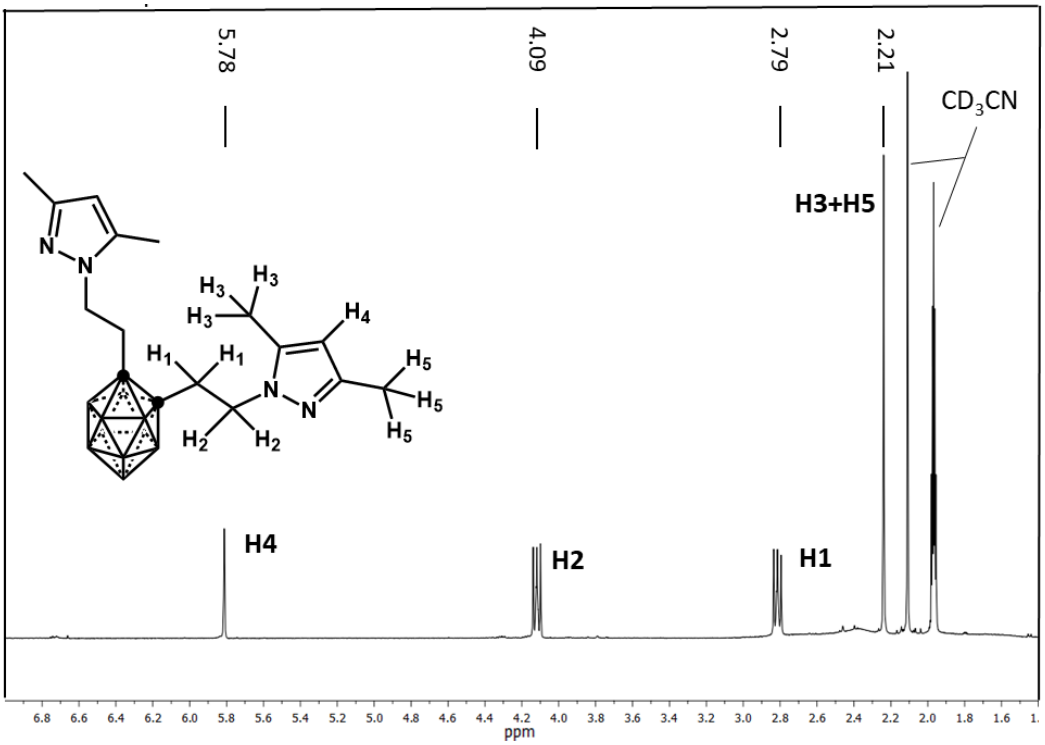

Figure S12. ^{1}H NMR spectrum of **L4** (CD_3CN, 400.0 MHz).

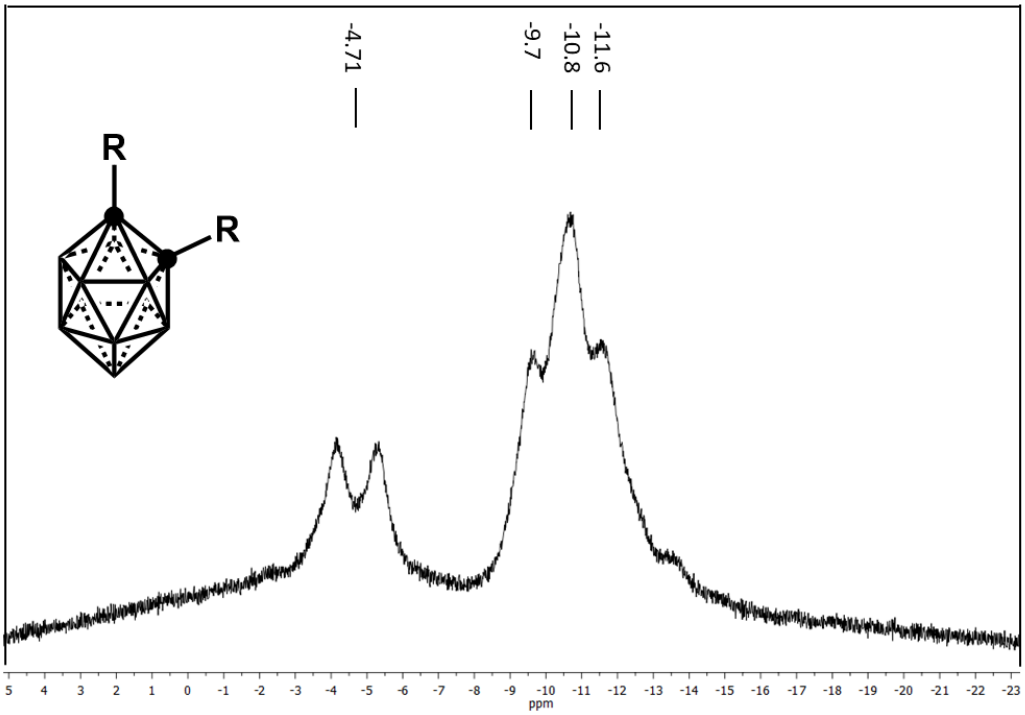

Figure S13. ^{11}B NMR spectrum of **L4** (CD3CN, 128.6 MHz).

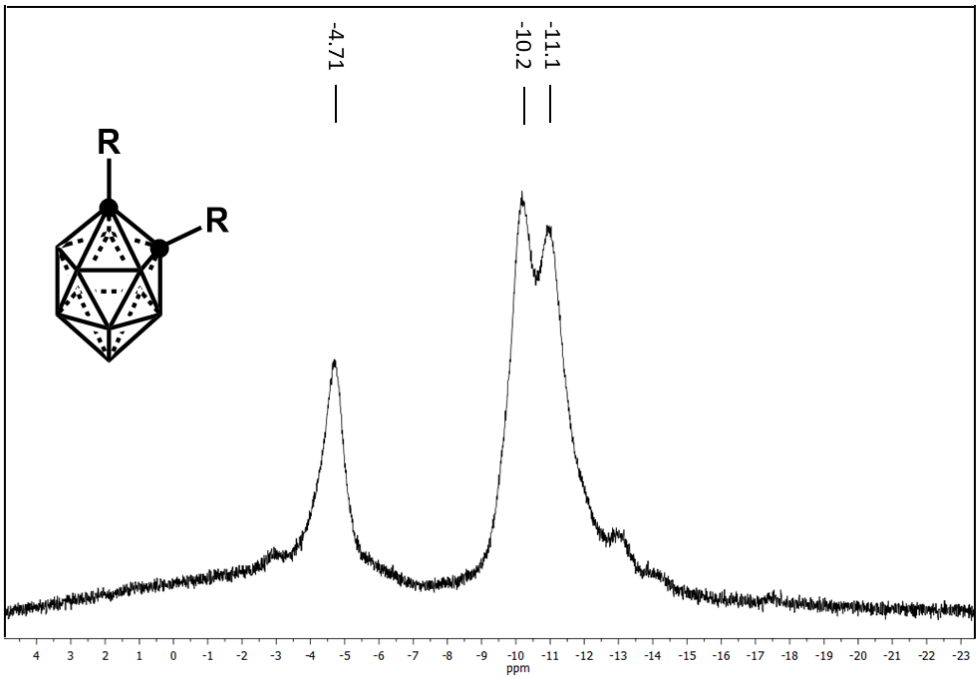

Figure S14. $^{11}B\{^{1}H\}$ NMR spectrum of **L4** (CD3CN, 128.6 MHz).

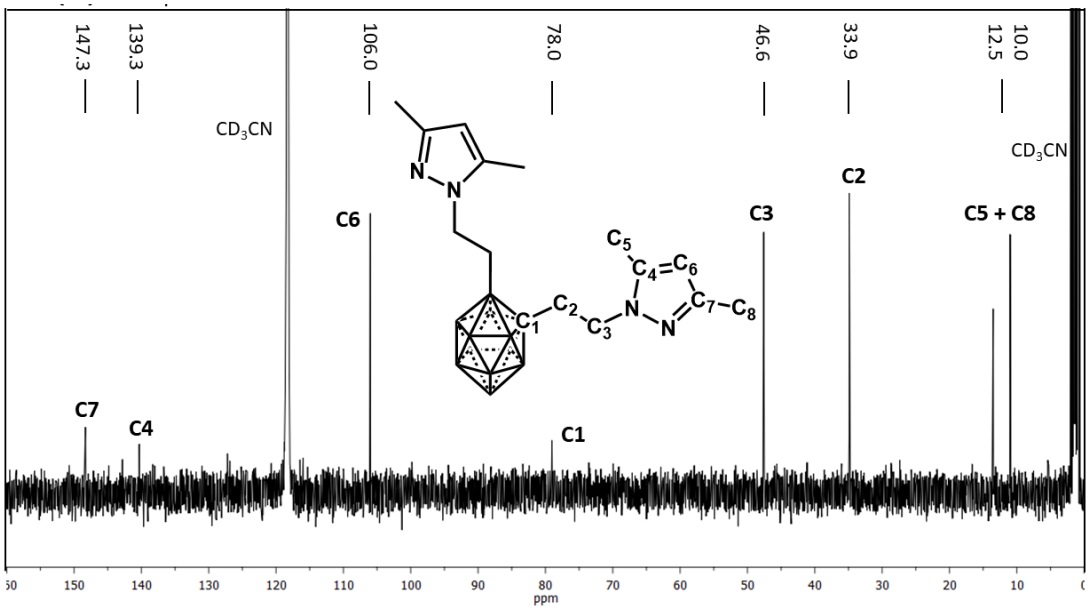

Figure S15. $^{13}C\{^{1}H\}$ NMR spectrum of **L4 (**CD_3CN, 100.6 MHz).

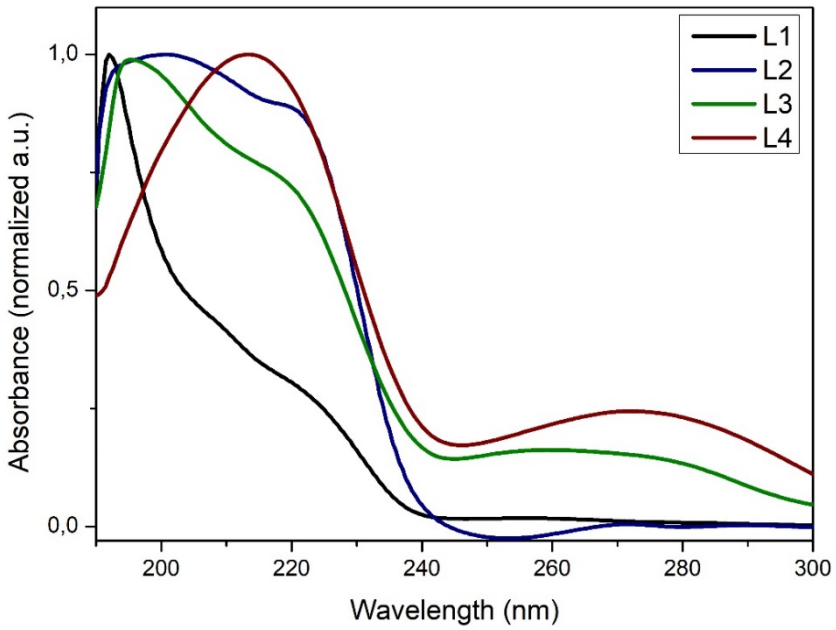

Figure S16. UV-Vis spectra of ligands **L1-L4** (CH_3CN, $1.45 \cdot 10^{-5}$ M to $6.5 \cdot 10^{-5}$ M, normalized spectra).

Crystallography for L3

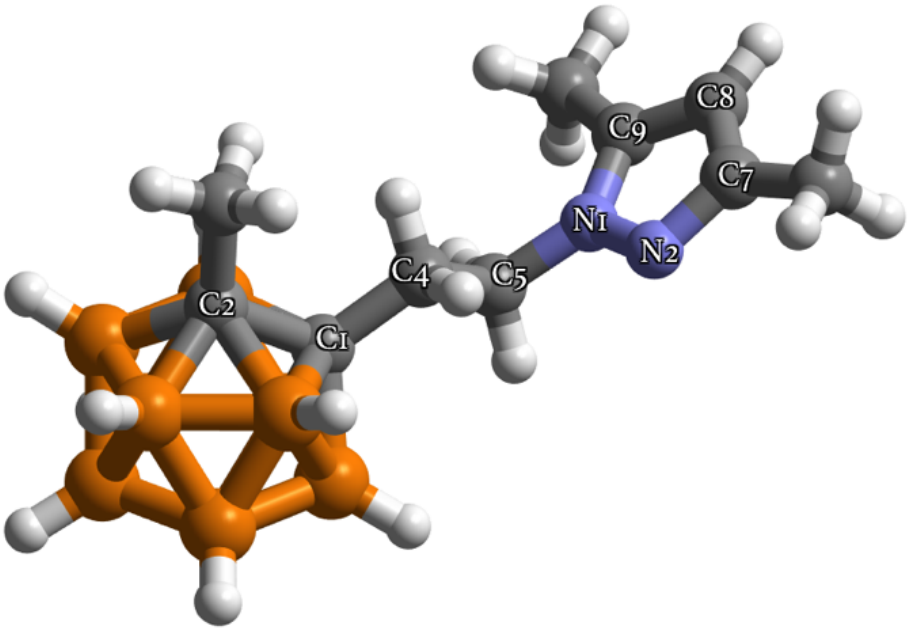

Figure S17. Molecular structure of **L3**; Selected interatomic distances (Å) and angles (º): C1–C2 1.6649(16), C1–C4 1.5267(15), C4–C5 1.5317(17), C5–N1 1.4509(15), N1–N2 1.3663(16), N2–C7 1.3364(17), C7–C8 1.399(3), C8–C9 1.384(2), C9–N1 1.3618(17), C1–C4–C5 113.42(10), C4–C5–N1 108.98(10), N1–N2–C7 104.61(12), N2–C7–C8 111.03(14), C7–C8–C9 106.38(12), C8–C9–N1 105.32(14). Color code: C (gray), H (white), B (orange), N (blue).

FTIR-ATR spectra for Compounds 1-4

The FTIR-ATR spectra of compounds **1-4** are similar to those of the parent ligands **L1-L4**, although slight differences in the region between 1600-500 cm^{-1} confirm the coordination of the metal centres to the ligands. They show characteristic bands for pyrazole groups such as [ν(C=C/C=N)$_{ar}$] (1556-1550 cm^{-1}), [δ(C=C/C=N)$_{ar}$] (1465-1417 cm^{-1}), [δ(C-H)$_{ip}$] (1049-1016 cm^{-1}) and [δ(C-H)$_{oop}$] (801-722 cm^{-1}).[1] For compounds containing carboranes, broad [ν(B-H)] bands centred at 2572-2563 cm^{-1} are identified.[1] The corresponding spectra can be seen in Figures S18-S21, with relevant signals highlighted in bold.

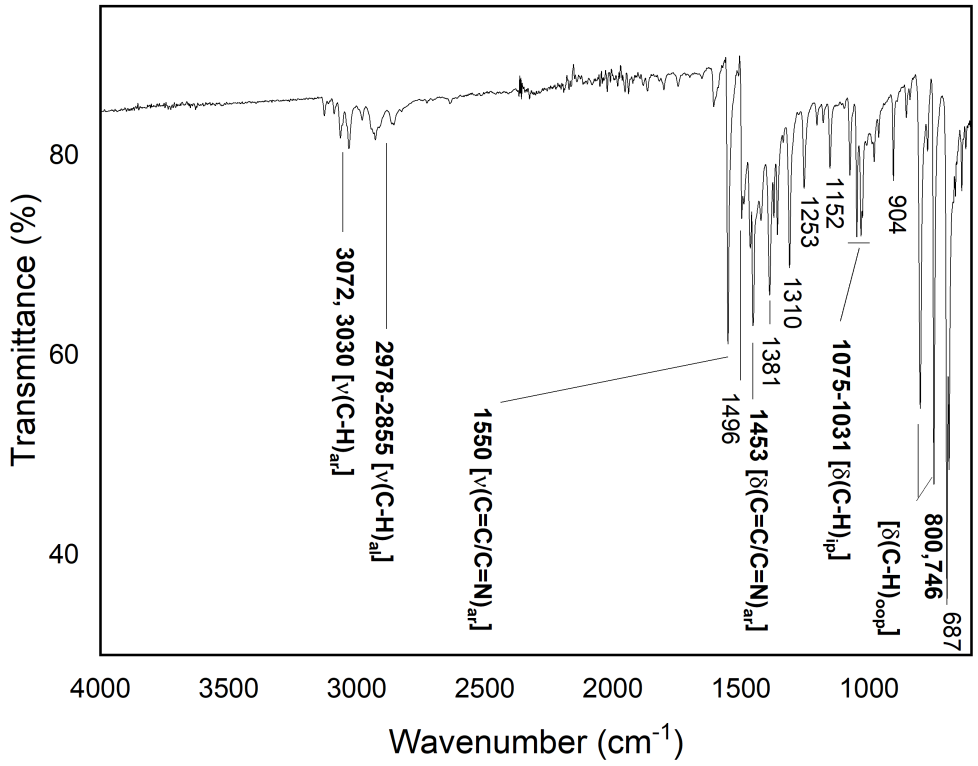

Figure S18. FTIR-ATR spectrum of compound [Cu(**L1**)I]$_n$ (**1**).

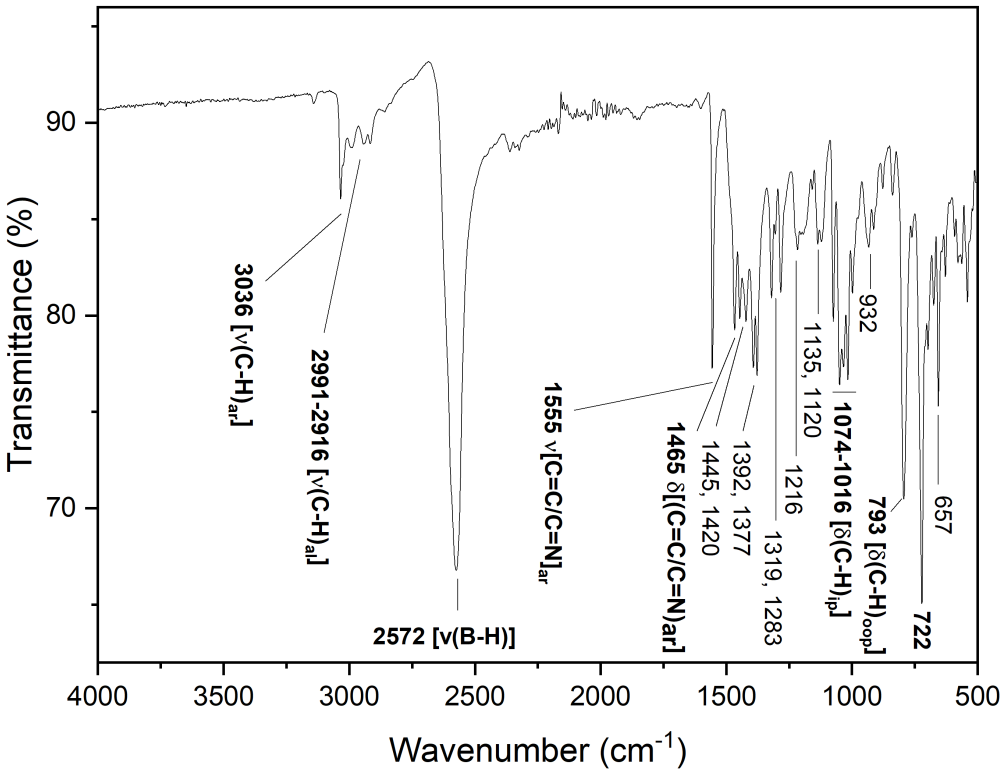

Figure S19. FTIR-ATR spectrum of compound [Cu(**L2**)I]$_2$ (**2**).

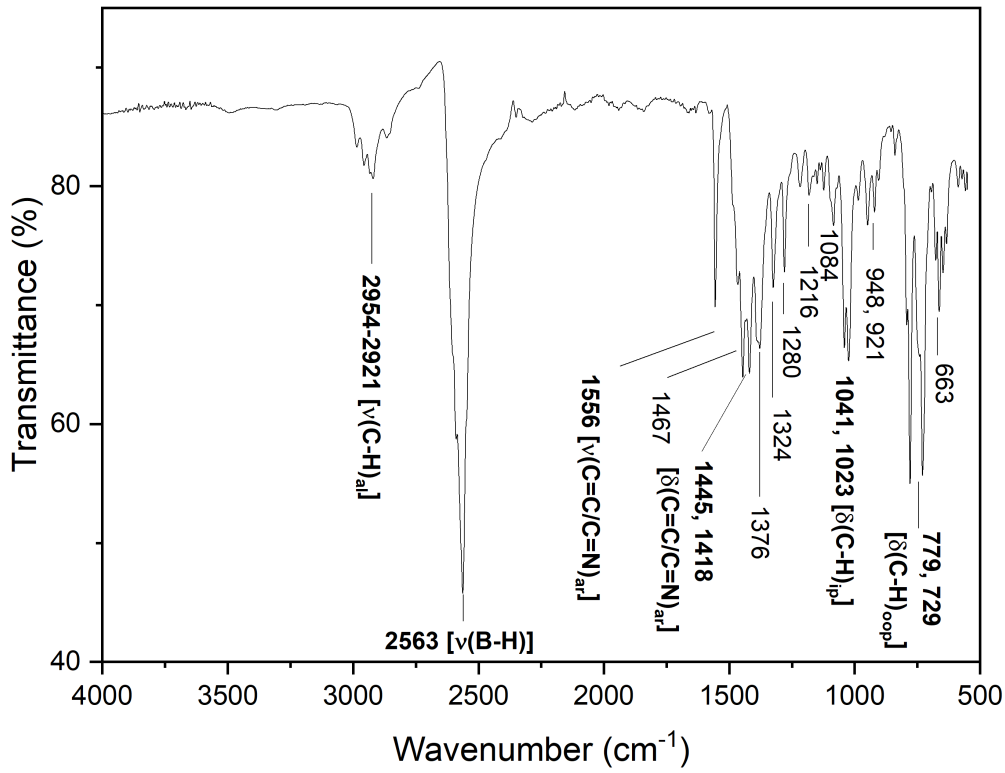

Figure S20. FTIR-ATR spectrum of compound [Cu(**L3**)I]$_4$ (**3**).

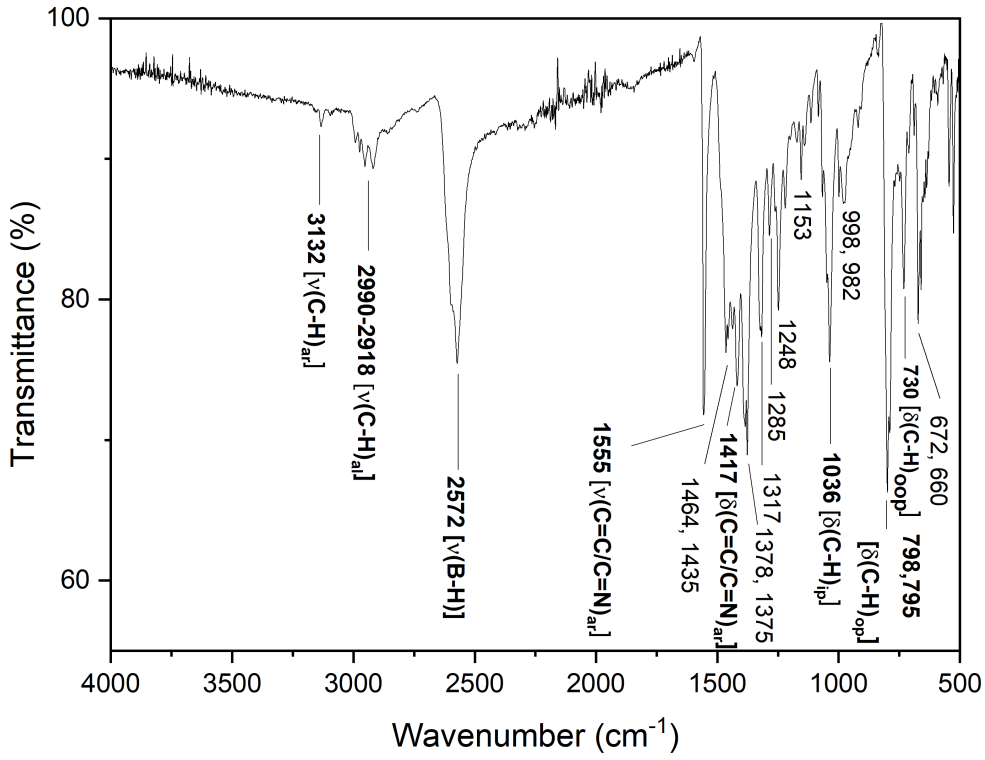

Figure S21. FTIR-ATR spectrum of compound $\{[Cu_4(\mathbf{L4})_2I_4]\cdot(CH_3CN)\}_n$ (**4**).

PXRD Patterns for Compounds 1, 2 and 4

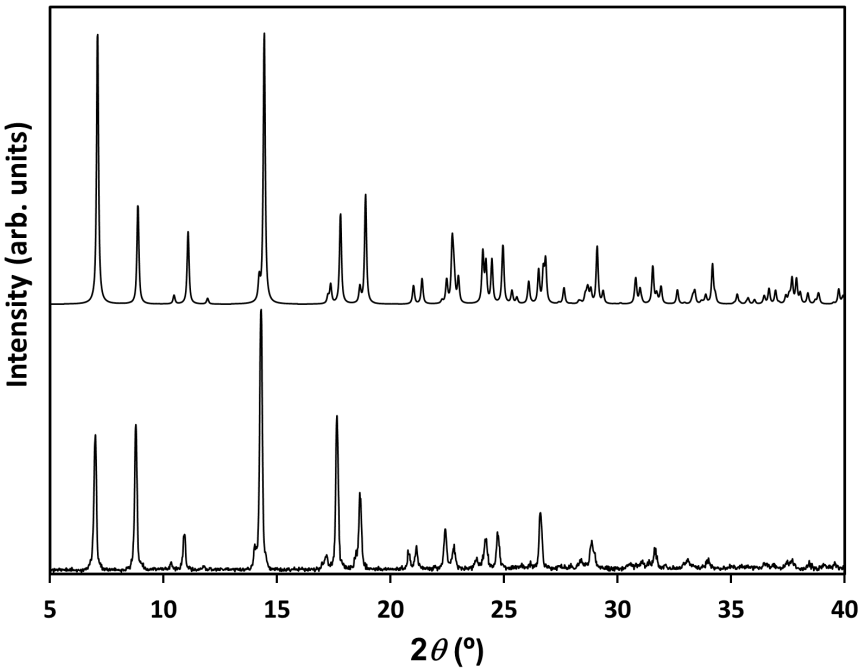

Figure S22. Calculated (top) and experimental (bottom) PXRD pattern of **1**.

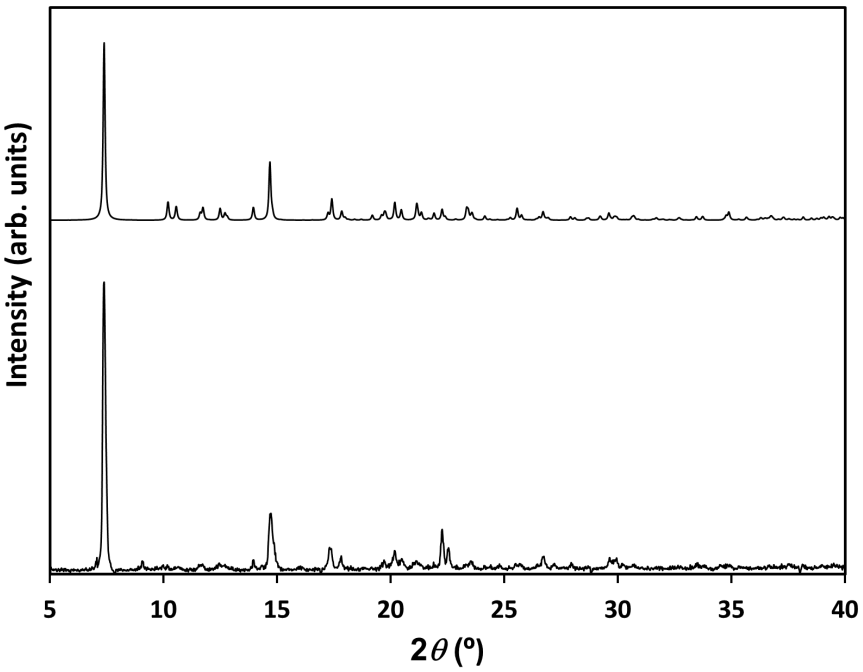

Figure S23. Calculated (top) and experimental (bottom) PXRD pattern of **2**.

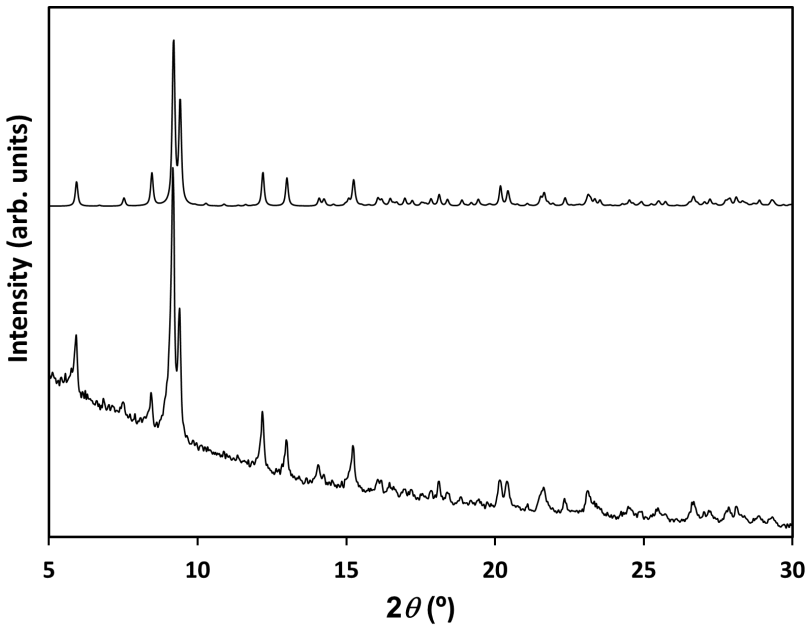

Figure S24. Calculated (top) and experimental (bottom) PXRD pattern of **4**.

NMR Spectra for compounds 2 and 3

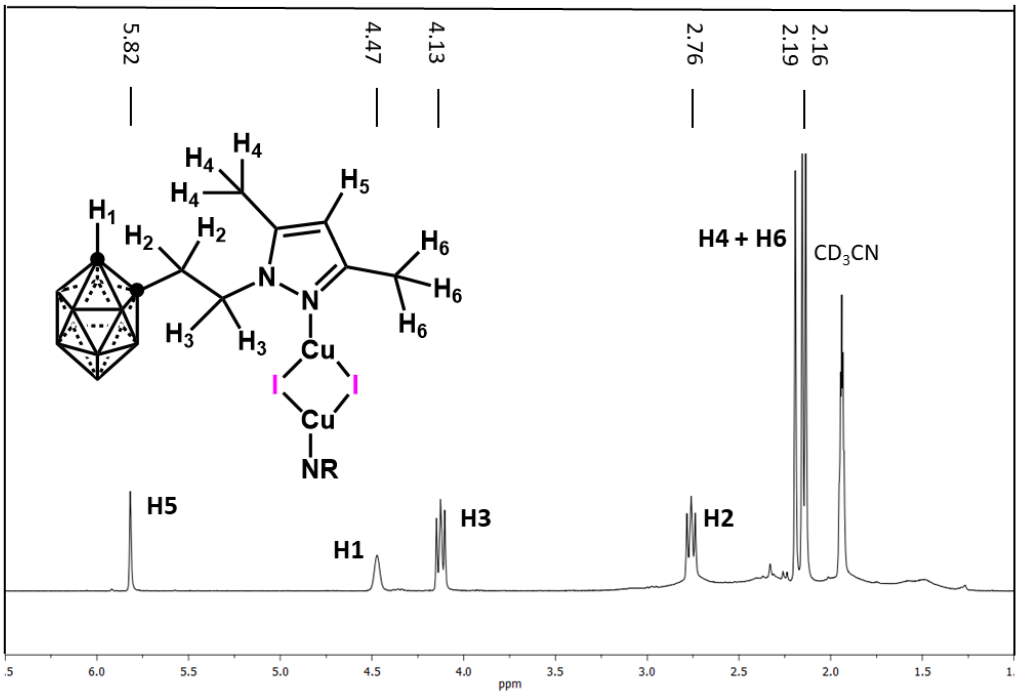

Figure S25. ^{1}H NMR spectrum of compound **2** (CD_3CN, 400.0 MHz).

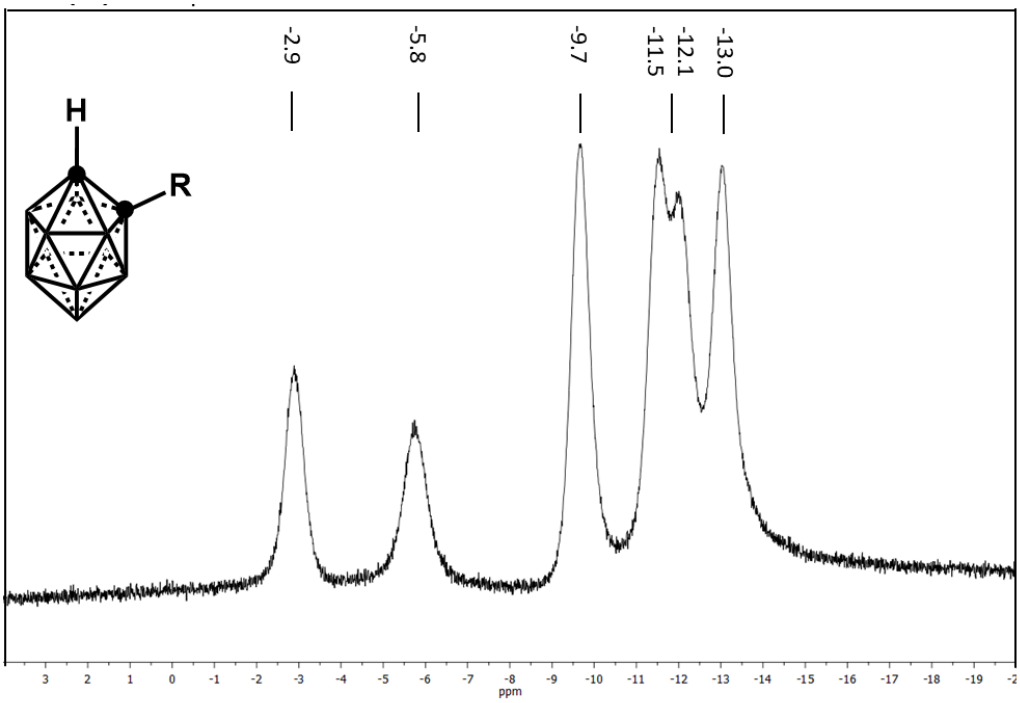

Figure S26. ^{11}B NMR spectrum of compound **2** (CD_3CN, 128.6 MHz).

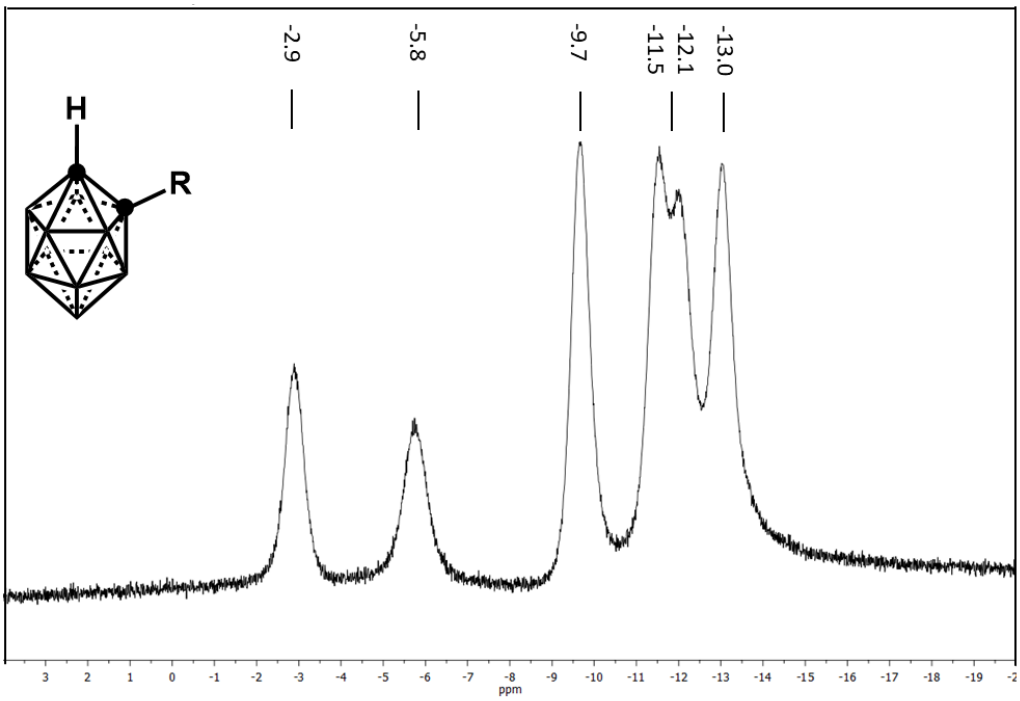

Figure S27. $^{11}B\{^{1}H\}$ NMR spectrum of compound **2** (CD_3CN, 128.6 MHz).

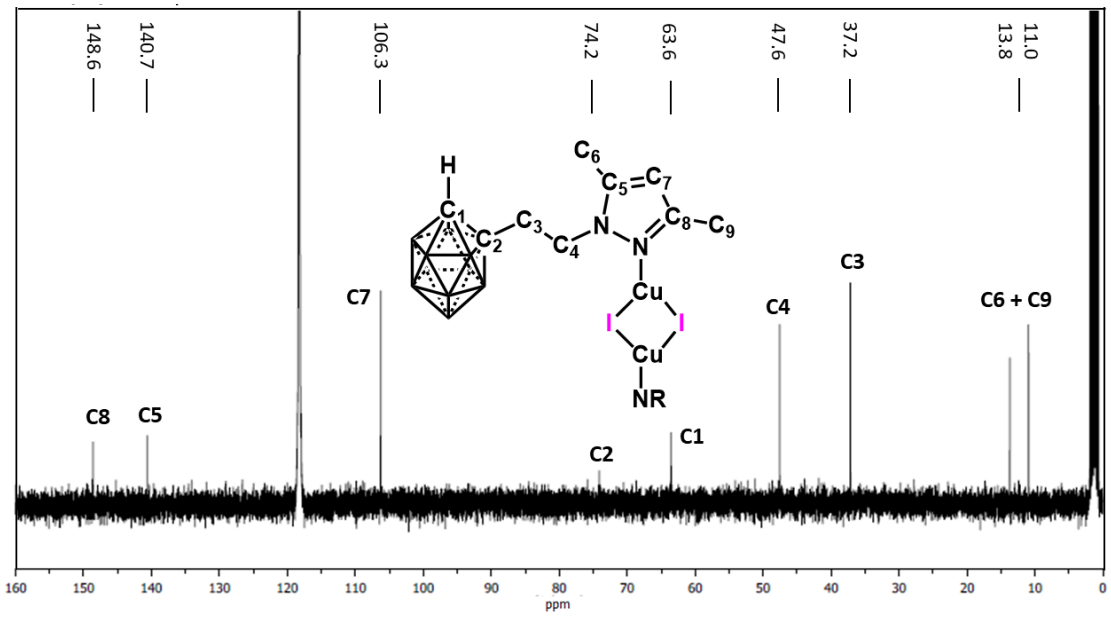

Figure S28. $^{13}C\{^{1}H\}$ NMR spectrum of compound **2** (CD_3CN, 100.6 MHz).

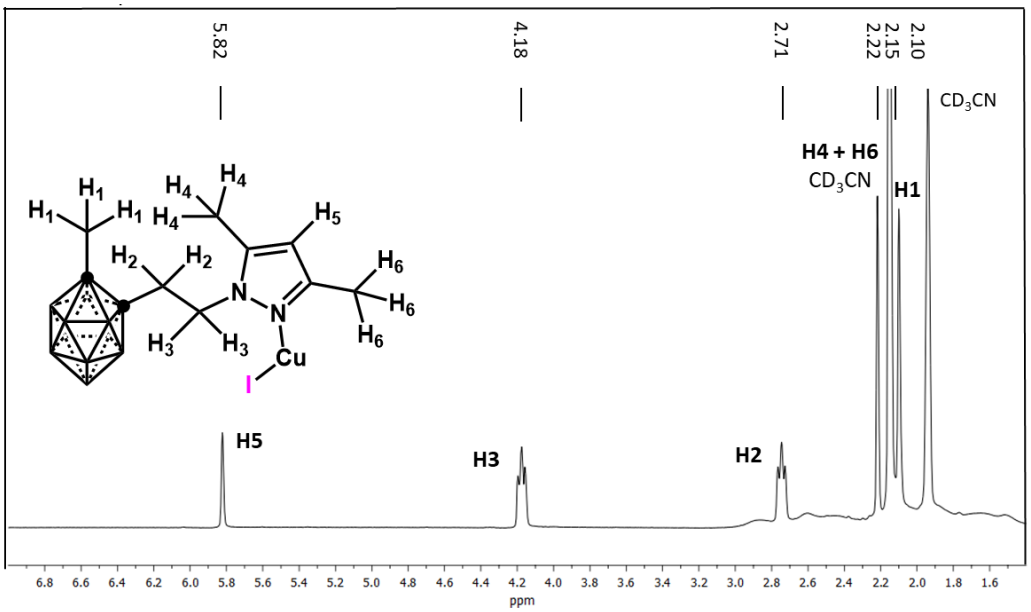

Figure S29. ^{1}H NMR spectrum of compound **3** (CD_3CN, 400.0 MHz)

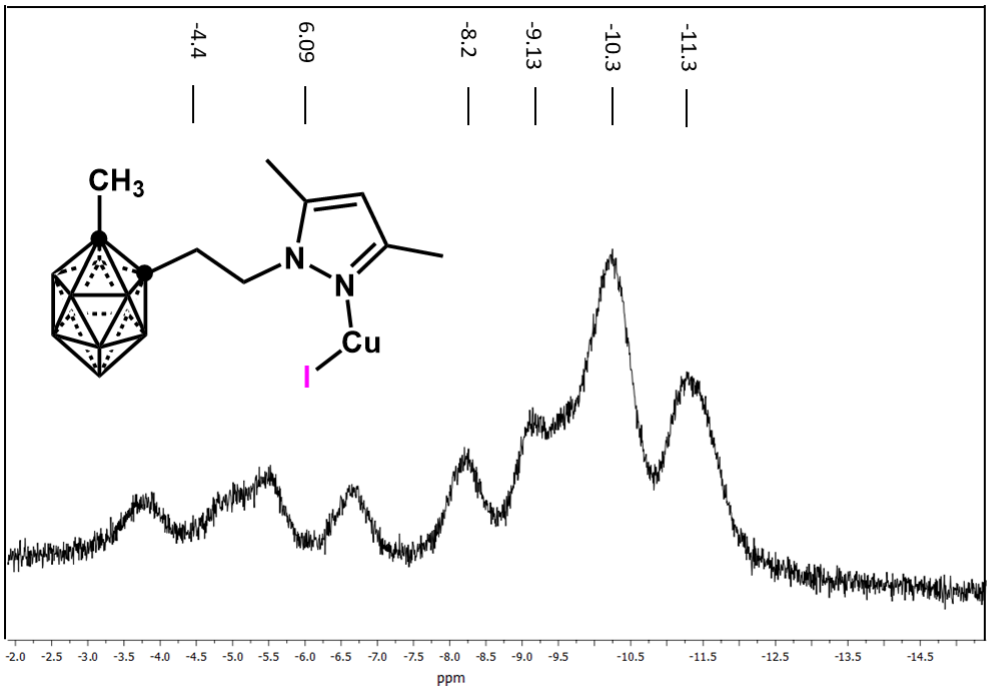

Figure S30. ^{11}B NMR spectrum of compound **3** (CD_3CN, 128.6 MHz).

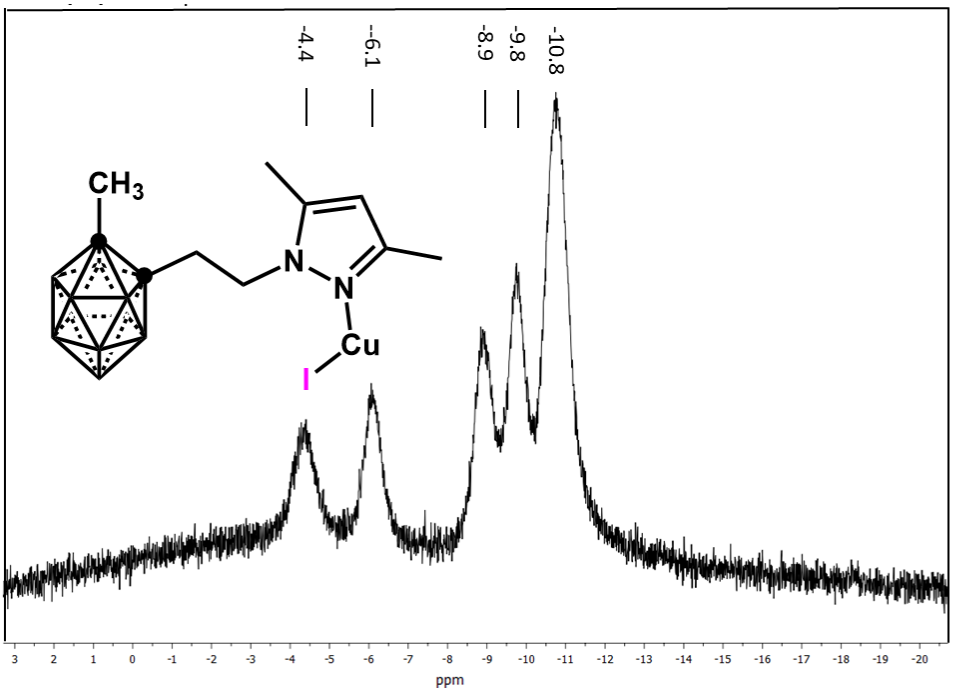

Figure S31. $^{11}B\{^{1}H\}$ NMR spectrum of compound **3** (CD_3CN, 128.6 MHz).

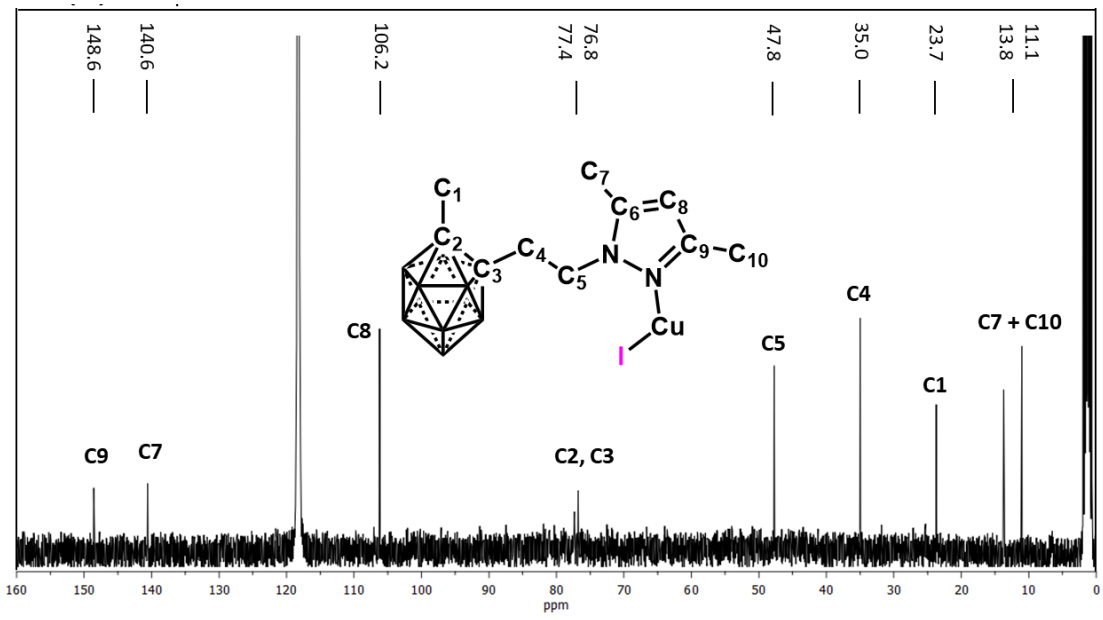

Figure S32. $^{13}C\{^{1}H\}$ NMR spectrum of compound **3** (CD_3CN, 100.6 MHz).

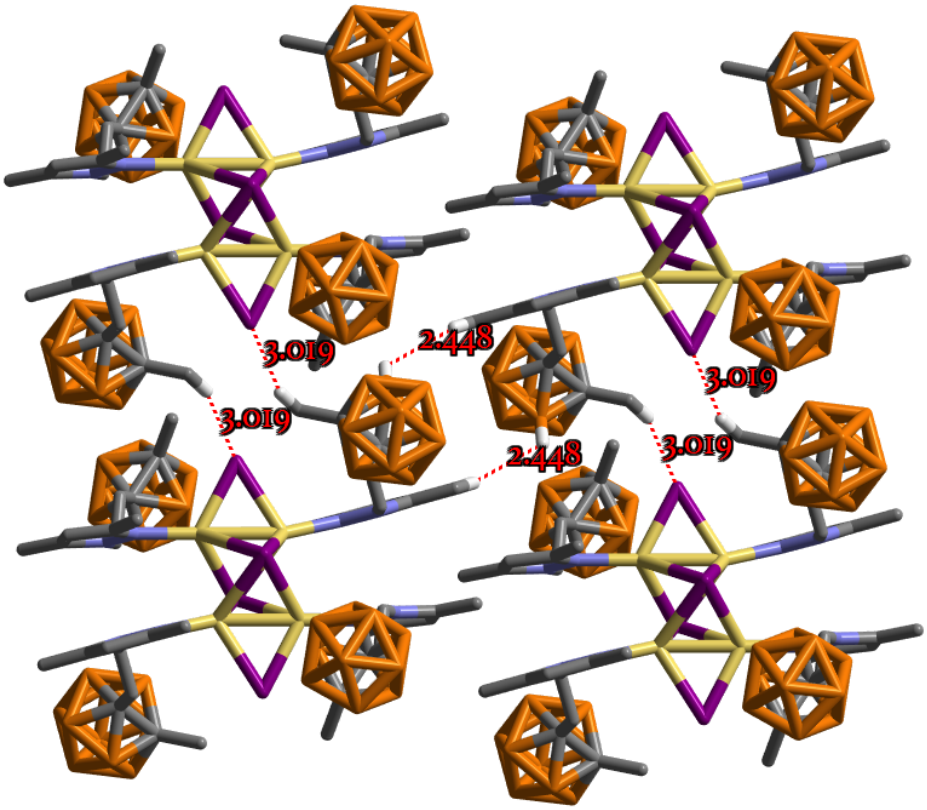

Figure S33. A perspective view of the packing of **3** showing the intermolecular contacts; C–H···I (H···I 3.019 Å, C–H···I 161.7º) and C–H···H–B (H···H 2.448 Å, C–H···H 130.5º, B–H···H 110.4º). Color code: C (gray), H (white), B (orange), N (blue), I (violet).

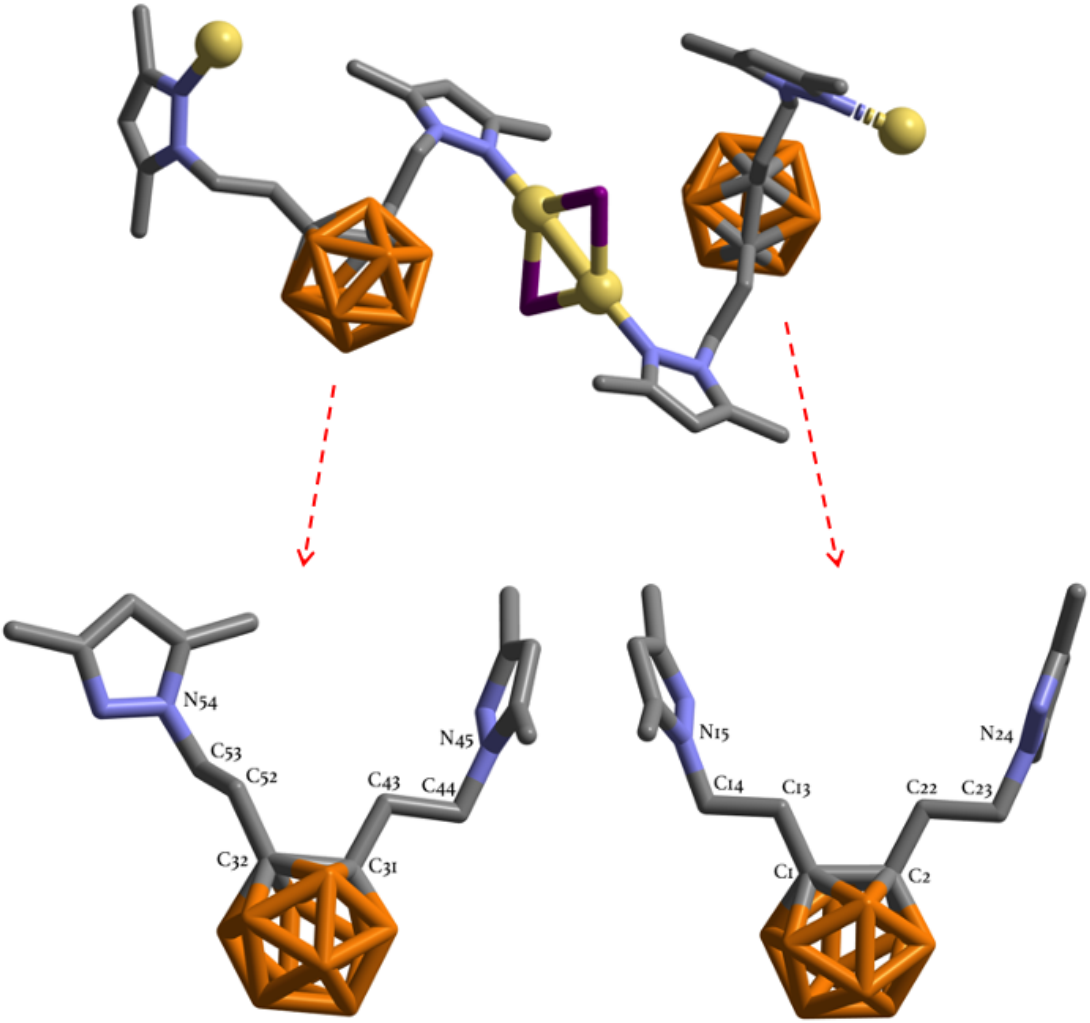

Figure S34. Top: Fragment of the 3D structure of **4** showing two carboranylpyrazole ligands in different conformations. Bottom: Detailed of the carboranyl pyrazole ligands' conformation with numbering scheme; Selected torsion angles (º): N45–C44–C43–C31 -170.9(4), C43–C31–C32–C52 -4.3(7), C32–C52–C53–N54 171.5(5) and N24–C23–C22–C2 171.8(4), C22–C2–C2–C13 0.4(7), C1–C13–C14–N15 -167.8(4); Angles between the pyrazole rings (º): 84.02 (left) and 42.76 (right). Color code: C (gray), B (orange), N (blue).

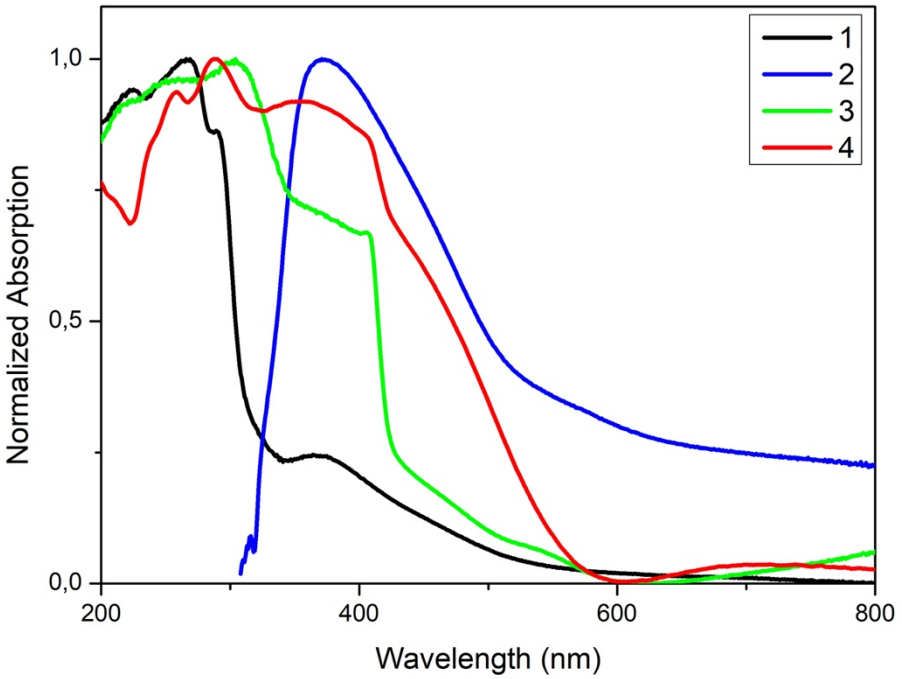

Figure S35. Solid state UV-Vis spectra of compounds **1**-**4** (normalized spectra).

Geometric Parameters of the compounds

Table S1. Bond lengths (Å) and angles (°) for compounds **1** and **2**.

1		**2**			
Bond lengths (Å)					
Cu(1)-I(1)	2.5538(6)	Cu(1A)-I(1A)	2.5426(7)	Cu(1B)-I(1B)	2.5439(7)
Cu(1)-I(1)#1	2.5499(6)	Cu(1A)-I(1A)#1	2.6084(7)	Cu(1B)-I(1B)#2	2.6107(7)
Cu(1)-N(1)	1.971(4)	Cu(1A)-N(21)	1.954(3)	Cu(1B)-N(21B)	1.963(3)
Cu(1)···Cu(1)	4.275	Cu(1A)···Cu(1A)#1	2.4726(9)	Cu(1B)···Cu(1B)#2	2.5158(9)
Bond angles (°)					
Cu(1)#1-I(1)-Cu(1)	113.77(2)	Cu(1A)#1-Cu(1A)-I(1A)	62.66(2)	Cu(1B)#2-Cu(1B)-I(1B)	62.12(2)
I(1)#2-Cu(1)-I(1)	113.78(2)	Cu(1A)#1-Cu(1A)-I(1A)#1	59.98(2)	Cu(1B)#2-Cu(1B)-I(1B)#2	59.46(2)
N(1)-Cu(1)-I(1)	120.31(11)	I(1A)-Cu(1A)-I(1A)#1	122.64(2)	I(1B)-Cu(1B)-I(1B)#2	121.59(2)
N(1)-Cu(1)-I(1)#2	125.88(11)	N(21A)-Cu(1A)-I(1A)	122.31(10)	N(21B)-Cu(1B)-I(1B)	124.68(8)
		N(21A)-Cu(1A)-I(1A)#1	114.99(9)	N(21B)-Cu(1B)-I(1B)#2	113.61(8)
		N(21A)-Cu(1A)-Cu(1A)#1	174.46(10)	N(21B)-Cu(1B)-Cu(1B)#2	172.26(9)
		Cu(1A)-I(1A)-Cu(1A)#1	57.36(2)	Cu(1B)-I(1B)-Cu(1B)#2	58.41(2)
#1: x+1, y, z #2 : x-1, y, z		#1: -x+1, -y+1, -z+1		#2: -x, -y+1, -z+2	

Table S2. Bond lengths (Å) and angles (°) for compound **3**.

3					
Bond lengths (Å)					
Cu(1)-I(1)	3.1044(8)	Cu(2)-I(1)	2.6985(6)	Cu(2)-N(52)	1.990(4)
Cu(1)-I(1)#1	2.7027(7)	Cu(2)-I(1)#1	2.7437(6)	Cu(1)-Cu(2)	2.5917(8)
Cu(1)-I(2)	2.5662(6)	Cu(2)-I(2)	2.6474(6)	Cu(1)-Cu(2)#1	2.9289(9)
Cu(1)-N(22)	1.984(4)				
Bond angles (°)					
Cu(2)-Cu(1)-Cu(2)#1	81.92(2)	N(22)-Cu(1)-I(1)	121.00(11)	N(52)-Cu(2)-Cu(1)	157.28(11)
Cu(2)-Cu(1)-I(1)	55.680(18)	N(22)-Cu(1)-I(2)	118.79(11)	N(52)-Cu(2)-I(1)	129.93(11)
Cu(2)-Cu(1)-I(1)#1	62.384(19)	Cu(1)-Cu(2)-Cu(1)#1	98.07(2)	N(52)-Cu(2)-I(1)#1	115.49(10)
Cu(2)#1-Cu(1)-I(1)	54.003(17)	Cu(1)-Cu(2)-I(1)	71.83(2)	N(52)-Cu(2)-I(2)	105.24(11)
I(1)#1-Cu(1)-Cu(2)#1	57.089(17)	Cu(1)-Cu(2)-I(1)#1	60.791(18)	Cu(1)#1-I(1)-Cu(1)	91.661(19)
I(1)#1-Cu(1)-I(1)	88.339(19)	Cu(1)-Cu(2)-I(2)	58.645(19)	Cu(1)#1-I(1)-Cu(2)#1	56.823(17)
I(2)-Cu(1)-Cu(2)#1	141.75(3)	I(1)-Cu(2)-Cu(1)#1	57.230(17)	Cu(2)-I(1)-Cu(1)	52.488(17)
I(2)-Cu(1)-Cu(2)	61.762(19)	I(1)#1-Cu(2)-Cu(1)#1	66.265(19)	Cu(2)#1-I(1)-Cu(1)	59.732(17)
I(2)-Cu(1)-I(1)	93.00(2)	I(1)-Cu(2)-I(1)#1	96.383(18)	Cu(2)-I(1)-Cu(1)#1	65.678(19)
I(2)-Cu(1)-I(1)#1	109.71(2)	I(2)-Cu(2)-Cu(1)#1	153.99(2)	Cu(2)-I(1)-Cu(2)#1	83.615(18)
N(22)-Cu(1)-Cu(2)	176.55(11)	I(2)-Cu(2)-I(1)	101.161(19)	Cu(1)-I(2)-Cu(2)	59.593(19)
N(22)-Cu(1)-Cu(2)#1	96.74(11)	I(2)-Cu(2)-I(1)#1	106.11(2)		
N(22)-Cu(1)-I(1)#1	119.52(10)	N(52)-Cu(2)-Cu(1)#1	100.27(11)		
#1: -x, -y+1, -z+1					

Table S3. Bond lengths (Å) and angles (°) for compound **4**.

4					
Bond lengths (Å)					
Cu(1)-I(1)	2.5523(9)	Cu(2)-N(60)	1.979(4)	Cu(4)-I(3)	2.5547(10)
Cu(1)-I(2)	2.5853(9)	Cu(3)-I(3)	2.6351(10)	Cu(4)-I(4)	2.5991(10)
Cu(1)-N(21)	1.966(4)	Cu(3)-I(4)	2.8614(9)	Cu(4)-N(30)#2	1.987(5)
Cu(2)-I(1)	2.5772(9)	Cu(3)-I(4)#1	2.7128(9)	Cu(1)-Cu(2)	2.5583(10)
Cu(2)-I(2)	2.5421(10)	Cu(3)-N(51)	1.998(4)	Cu(3)-Cu(4)	2.6373(12)
Bond angles (°)					
Cu(2)-Cu(1)-I(2)	59.23(3)	N(21)-Cu(1)-I(2)	122.77(13)	Cu(4)-Cu(3)-I(4)#1	81.53(3)
I(1)-Cu(1)-I(2)	119.55(3)	I(2)-Cu(2)-I(1)	120.26(3)	Cu(4)-Cu(3)-I(4)	56.24(3)
N(21)-Cu(1)-Cu(2)	175.11(14)	N(60)-Cu(2)-Cu(1)	173.37(15)	I(3)-Cu(3)-Cu(4)	57.97(3)
N(21)-Cu(1)-I(1)	117.67(13)	N(60)-Cu(2)-I(1)	114.33(15)	I(3)-Cu(3)-I(4)	107.66(3)
I(2)-Cu(2)-Cu(1)	60.91(3)	N(60)-Cu(2)-I(2)	125.34(15)	I(3)-Cu(3)-I(4)#1	103.59(3)
I(1)-Cu(1)-Cu(2)	60.57(3)	Cu(1)-Cu(2)-I(1)	59.60(3)	I(4)#1-Cu(3)-I(4)	93.48(3)
N(51)-Cu(3)-Cu(4)	152.84(13)	N(51)-Cu(3)-I(3)	112.84(13)	N(51)-Cu(3)-I(4)#1	125.20(13)
N(51)-Cu(3)-I(4)	111.61(13)	I(3)-Cu(4)-Cu(3)	60.97(3)	I(3)-Cu(4)-I(4)	118.94(3)
I(4)-Cu(4)-Cu(3)	66.24(3)	N(30)#2-Cu(4)-Cu(3)	170.21(18)	N(30)#2-Cu(4)-I(3)	119.77(14)
N(30)#2-Cu(4)-I(4)	117.54(14)	Cu(1)-I(1)-Cu(2)	59.83(2)	Cu(2)-I(2)-Cu(1)	59.85(2)
Cu(4)-I(3)-Cu(3)	61.06(3)	Cu(3)#1-I(4)-Cu(3)	86.52(3)	Cu(4)-I(4)-Cu(3)#1	77.50(3)
Cu(4)-I(4)-Cu(3)	57.52(3)				
#1 -x,-y+2,-z+1 #2 -x+1,y+1/2,-z+3/2 #3 -x+1,y-1/2,-z+3/2					

Table S4. Comparison of relevant bond lengths for compounds **1-4**

	Schematic representation of the *core* geometrical motif	Cu-N bond lengths (Å) **(Mean value)**	Cu-I bond lengths (Å) **(Mean value)**	Cu-Cu bond lengths (Å) **(Mean value)**
1	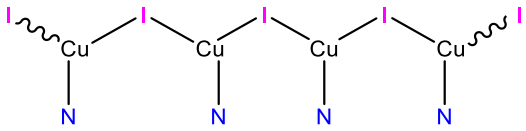	1.971(4)	2.5538(6) 2.5499(6) **2.5520(6)**	4.275
2	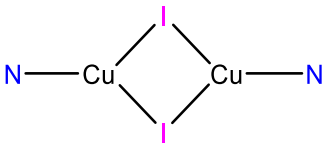	1.9543(3) 1.963(3) **1.958(3)**	2.5426(7) 2.6084(7) 2.5439(7) 2.6107(7) **2.5764(7)**	2.4726(9) 2.5158(9) **2.4942(9)**
3	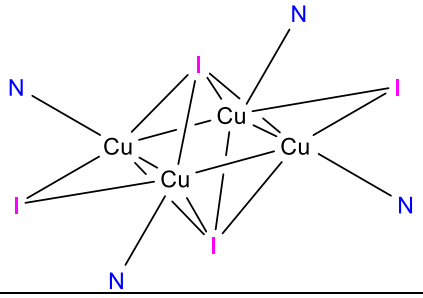	1.984(4) 1.990(4) **1.987(4)**	3.1044(8) 2.7027(7) 2.5662(6) 2.6985(6) 2.7437(6) 2.6474(6) **2.7438(7)**	2.5917(8) 2.9289(8) **2.7603(8)**
4	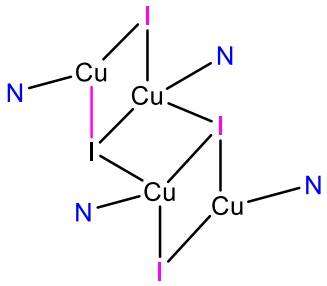	1.998(4) 1.987(5) **1.993(5)**	2.6351(10) 2.8614(9) 2.7128(9) 2.5547(10) 2.5991(10) **2.6726(10)**	2.6373(12)
	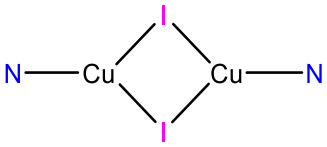	1.966(4) 1.979(4) **1.973(4)**	2.5523(9) 2.5853(9) 2.5772(9) 2.5421(10) **2.5590(9)**	2.5583(10)

References

1 K. Nakamoto, *Handb. Vib. Spectrosc.*, 2006, 1872–1892.